

# Synthesis of Ag/ZIF-67 as a Heterogeneous Catalyst for Methyl Orange Degradation in Presence of H<sub>2</sub>O<sub>2</sub>

Pham Quoc Yen<sup>1</sup>, Le Thi Anh Thu<sup>1</sup>, Pham Van Toan<sup>2</sup>, Ho Ngoc Tri Tan<sup>3</sup>,  
Dang Huynh Giao<sup>1,\*</sup>

<sup>1</sup>Department of Chemical Engineering, College of Engineering Technology, Can Tho University, Vietnam

<sup>2</sup>Department of Environmental Engineering, College of Environment and Natural Resources, Can Tho University, Vietnam

<sup>3</sup>Department of Civil Engineering, College of Engineering Technology, Can Tho University, Vietnam

**Abstract**— A metal-organic framework Ag/ZIF-67 was successfully synthesized and characterized by several methods including X-ray powder diffraction (PXRD), Fourier transform infrared (FT-IR), Scanning electron microscopy (SEM), and Thermogravimetric analysis (TGA). The results showed that Ag/ZIF-67 had a polyhedron structure was similar with ZIF-67 and 5.1% of Ag nanoparticles was loaded into its structure. The catalytic activity of Ag/ZIF-67 was then investigated into methyl orange (MO) mineralization process in presence of H<sub>2</sub>O<sub>2</sub>. High efficiency was obtained with over 99% when using H<sub>2</sub>O<sub>2</sub> concentration 0.08 mol.L<sup>-1</sup>, methyl orange concentration 10 mg.L<sup>-1</sup>, Ag/ZIF-67 concentration 200 mg.L<sup>-1</sup> at 30°C, pH 7 in 180 min. The solid and could be recycled and reused without a significant degradation in catalytic activity with the efficiency is over 90% after 3 times.

**Keywords**— Synthesis, Ag/ZIF-67, methyl orange degradation, H<sub>2</sub>O<sub>2</sub>, catalyst, solution impregnation.

## I. INTRODUCTION

Metal-organic frameworks (MOFs) are a class of porous coordination polymers (PCPs), promising crystalline solid-state materials [1]. Zeolitic imidazolate frameworks (ZIFs) is one group of MOFs, built by transition metal (such as Zn or Co) and imidazole compounds as lattice nodes and bridges, respectively [2]. Compared to other types of MOFs materials, ZIFs would be illustrated remarkable properties that are better thermal, hydrothermal and chemical stabilities [3, 4].

Recently, loading metal nanoparticles (NPs) techniques into ZIFs have been more and more interesting, seeing that ZIFs are shown to be suitable capability as matrices to encapsulate and support functional NPs [5]. This combination would be important development for catalyst manufacture owing to taking full the best characteristic of NPs and host matrix, maybe they can increase electrical and catalyst properties to prepare with single component material [6].

In recent years, several examples of incorporation of NPs into cavities of ZIFs systems have been reported by difference methods for preparation, such as doping Au, Pt, Ni, Pd into ZIF-8 and ZIF-90 [7-10], encapsulating Ag, Pd, Cu by ZIF-67 core-shell [6, 11-13]. NPs-ZIFs have demonstrated application potentials for catalyst and decontamination [14, 15]. For instance, Han-Qing Yu (2013) investigated to synthesize Pd@ZIF-67 that was used as heterogeneous catalyst for Cr(IV) reduction to Cr(III). In detail, the PdNPs were embedded into ZIF-67 via two periods: (i) firstly, palladium acetate (Pd(OAc)<sub>2</sub>) impregnated with ZIF-67 through material's channel; (ii) subsequently, Pd<sup>2+</sup> would reduce to Pd zero valent by HCOOH. This material showed high catalytic performance and could be reused for ten times [6].

Methyl orange (MO) is an azoic organic dye that is broadly consumed in industry. Like many other dyes of its class MO on inadvertently entering the body through ingestion, metabolizes into aromatic amines by intestinal

microorganisms [16]. It is also demonstrated to have acute toxicity to humans and ecosystems. To date, many methods have been carried out to decontaminated the present of MO in wastewater such as Fenton processes [17, 18], H<sub>2</sub>O<sub>2</sub>/UV [19]. They would be shown effective solution but the oxidizing agent or catalyst of those methods is not able to recycle. In this paper, we propose the process to mineralize MO using Ag/ZIF-67 in presence of H<sub>2</sub>O<sub>2</sub>. This method is also based on the attack of hydroxyl radicals ( $\dot{\text{O}}\text{H}$ ) on MO. Hydroxyl radicals work as extremely strong oxidizing agents with  $E^0 = 2.8 \text{ V/NHE}$  at room temperature and atmospheric pressure [19], which is created by the catalysis of Ag NPs on ZIF-67 surface for H<sub>2</sub>O<sub>2</sub> decomposition. Here we report a new method to prepare Ag/ZIF-67, its catalytic capacity for MO degradation and affective factors on this process.

## II. MATERIALS AND METHODS

### A. Material

Cobalt (II) nitrate hexahydrate (Co(NO<sub>3</sub>)<sub>2</sub>·6H<sub>2</sub>O) 99.99%, 2-methylimidazole (C<sub>4</sub>H<sub>6</sub>N<sub>2</sub>) 99%, methanol, silver nitrate (AgNO<sub>3</sub>) >99%, formic acid (HCOOH), acetone (CH<sub>3</sub>COCH<sub>3</sub>) were purchased from Sigma-Aldrich, methyl orange (C<sub>14</sub>H<sub>14</sub>N<sub>3</sub>NaO<sub>3</sub>S), hydrogen peroxide (H<sub>2</sub>O<sub>2</sub>) were purchased from Xi long scientific Co., Ltd, China.

### B. Preparation of ZIF-67

ZIF-67 was synthesized according to previous report with the ratio of Co<sup>2+</sup> and 2-HMim is 1:4 [6, 20]. Briefly, 0.717 g cobalt nitrate hexahydrate (0.0025mol) and 0.821 g 2-methyl imidazole (0.01mol) were respectively dissolved in 25 mL methanol. Then 2-methyl imidazole solution was gradually added into cobalt salt solution. The mixture was stirred by magnetic stirring during 10 mins, and aged at ambient temperature over 24 h. After that, the purple precipitation was obtained by centrifugation at 6000 rpm within 8 mins. The

purple solid was washed by methanol (3x10 mL) for 3 days. Finally, the sample was dried at 60°C within 24 h.

### C. Encapsulation of AgNPs into ZIF-67

To synthesize the Ag/ZIF-67-1:4 (name code means the ratio of AgNO<sub>3</sub> doped amount and ZIF-67 is 1:4), 62.5 mg AgNO<sub>3</sub> was dissolved in 50 mL acetone obtaining transparent solutions. Then 250 mg ZIF-67 was added into the solution under magnetic stirring for 1 h [6]. Subsequently, 0.25 mL formic acid was added into the mixture at 60°C during 60 mins. The black solid rapidly precipitated, and separated solvent by Pasteur pipette. The obtained solid was washed with acetone several times and dried at 60°C within 8 h to get the major product. The preparations of Ag/ZIF-67-1:2, Ag/ZIF-67-1:1 and Ag/ZIF-67-2:1 were similar with that of Ag/ZIF-67-1:4 except for that the amount of AgNO<sub>3</sub> salt and HCOOH were changed.

### D. Catalyst experiments

Ag/ZIF-67 sample was dispersed into 50 mL methyl orange (MO) aqueous solution. The mixture was stirred within 1 h to establish the adsorption equilibrium of MO onto the surface of Ag/ZIF-67. Then H<sub>2</sub>O<sub>2</sub> 30% was added. The solution was continuously stirred for 30, 60, 90, 120, 150 and 180 mins at room temperature, respectively. After each period time, the solution was measured the absorbance of MO by UV-vis spectrophotometer. Effective factors to degradation process were observed including AgNO<sub>3</sub> doped amount, Ag/ZIF-67 dosage, initial concentration of MO, concentration of H<sub>2</sub>O<sub>2</sub>, time and temperature.

## III. RESULTS AND DISCUSSION

### A. Characterization of the Ag/ZIF-67

The Ag/ZIF-67 in ratio differences between the ZIF-67 and AgNO<sub>3</sub> were measured by XRD patterns to confirm crystalline structure. The result was showed in Fig.1. The sharp and clear peaks at 38°, 44°, 64°, 77° were detected in all samples, which were indexed for 4 planes 111, 200, 220 and 311, respectively of the face centered cubic silver [21]. However, almost peaks of ZIF-67 were not appeared when compared with PXRD of ZIF-67, it would be possible that the Ag NPs were grown along the direction and cover surface of ZIF-67 framework [6].

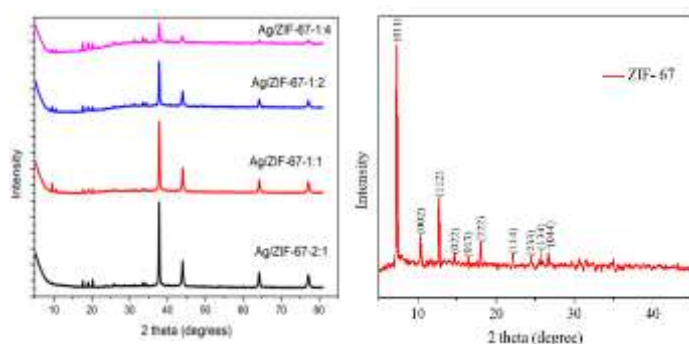


Fig. 1. Powder XRD patterns of Ag/ZIF-67 samples with ratio differences between AgNO<sub>3</sub> doped amount and ZIF-67

Additionally, the element component was analyzed by energy dispersive X-ray (EDX) spectra (Fig. 2). They verified the presence of corresponding elements in the representative Ag/ZIF-67-1:4 sample and quantified EDX spectroscopic data show that was loaded 5.1% of AgNPs.

Figure 3 showed the SEM micrographs of representative Ag/ZIF-67-1:4 sample (a) and ZIF-67 (b), respectively. The Ag/ZIF-67-1:4 sample had a polyhedron structure which was similar with ZIF-67 and reveal that these polyhedron possessed well- identified planes, direct margin and coarse surfaces.

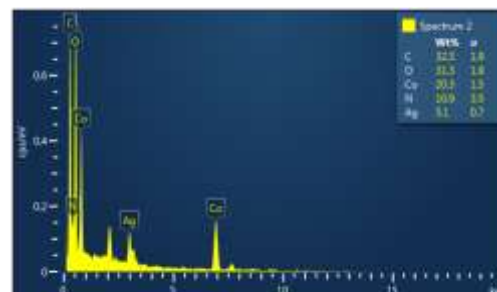


Fig. 2. EDX spectra of representative Ag/ZIF-67-1:4 sample

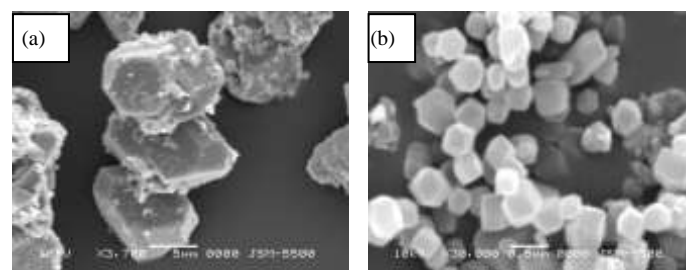


Fig. 3. SEM micrographs of representative Ag/ZIF-67-1:4 sample (a) and ZIF-67 (b)

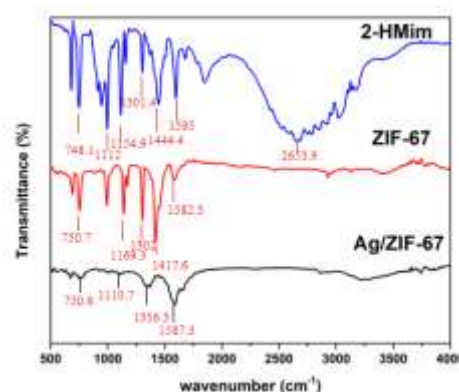


Fig. 4. FT-IR of 2-HMim, ZIF-67 and representative Ag/ZIF-67-1:4

To investigate surface chemistry of Ag/ZIF-67 the FT-IR spectrum was used and displayed in Fig.4. The spectrum of synthesized ZIF-67 appeared peaks from 600 cm<sup>-1</sup> to 1500 cm<sup>-1</sup> could be indicated to the stretching and bending frequency of the imidazole ring [22, 23]. The peak at 1582.3 cm<sup>-1</sup> could be a assigned of stretching mode of C=N bonding in ligand which deviate from the report of Lin *et al* (1584 cm<sup>-1</sup>) [22]. Since ZIF-67 was embedded by AgNPs (Ag/ZIF-67), position of these peaks was altered. Specifically, the stretching mode of C=N bonding in Ag/ZIF-67 was detected at 1587.3 cm<sup>-1</sup>

(deviating 5 cm<sup>-1</sup> from ZIF-67). Furthermore, Thermal gravimetric analysis (TGA) measurement was carried out from 50 to 800°C (Fig. 5). The TGA trace for ZIF-67 revealed a high decomposition temperature of 350°C while that of Ag/ZIF-67 is approximately 225°C. The reduction to initial decomposition temperature of ZIF-67 that might be due to high thermal conductivity property of Ag covered onto ZIF-67 surface.

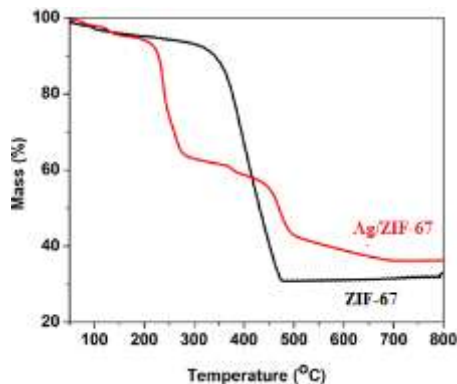


Fig. 5 TGA of representative Ag/ZIF-67-1:4 sample and ZIF-67.

### B. Catalyst Activities Evaluation

In this study, the hydroxyl radicals are generated by the catalysis of AgNPs in ZIF-67 surface with H<sub>2</sub>O<sub>2</sub> according to path way [24]:



the reaction (1) would be considered as the Fenton process, high oxidizing agent  $\cdot\text{OH}$  radicals continuously attack and mineralize dye molecular. The pathway for MO degradation based on report of Guivarch *et al* [17] is proposed in Fig.6.

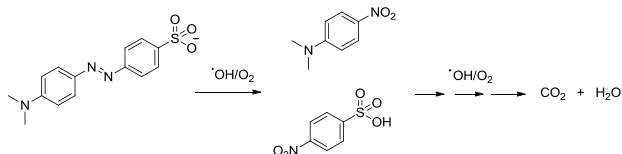


Fig. 6 Suggested reaction pathway for the degradation of MO by H<sub>2</sub>O<sub>2</sub>-Ag/ZIF-67

Temperature is crucial effective factor to a chemical reaction. In this work, experiments were conducted in a temperature range of 20-50°C to investigate the effect of temperature on the mineralization MO process. The results was shown in Fig. 7. It is observed that the degradation rates at 40°C and 50°C are faster than those at 20°C and 30°C, with decolorization efficiency at 60% within 30 min. However, the degradation of MO was not completed within 180 min. On the other hand, even though the degradation rate was quite slow at 20°C, the decolorization efficiency was more completely than that of 40°C and 50°C with approximately 90% within 180 min. The line of 30°C tended to have a trend between low and high temperature and achieved equilibrium within 90 min with degradation efficiency 85%. It is obviously proved that the temperature promotes degradation rate. At the same time, it also has some disadvantages because the temperature could boost the decomposition of H<sub>2</sub>O<sub>2</sub> lead to produce more  $\cdot\text{OH}$  radicals. As we known,  $\cdot\text{OH}$  can attack H<sub>2</sub>O<sub>2</sub> as Eq (2), therefore, it would reduce total efficiency.



To evaluate the effect of initial MO concentration on the decolorization efficiency, the variation of MO concentration was altered from 10 mg.L<sup>-1</sup> to 30 mg.L<sup>-1</sup>, and the result was illustrated in Fig.8. As the MO concentration increased, the degradation process rate rapidly increased within 30 min. Generally, MO molecular were adsorbed onto material surface before mineralized by  $\cdot\text{OH}$ . When MO concentration increased, the absorption efficiency was promoted since MO molecular easily diffuse to Ag/ZIF-67 surface, thus  $\cdot\text{OH}$  radicals just formed in Ag/ZIF-67 surface easy attack and break up MO molecular.

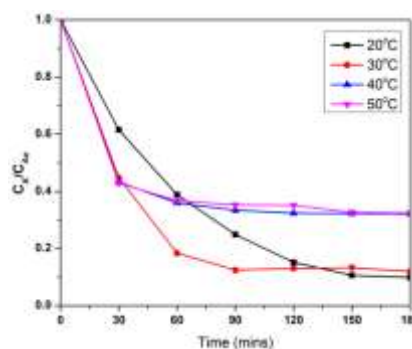


Fig. 7. Effect of temperature on the degradation efficiency of MO: initial MO concentration, 10 mg.L<sup>-1</sup>; Ag/ZIF-67 dose, 0.2 g.L<sup>-1</sup>; initial pH 7, H<sub>2</sub>O<sub>2</sub> concentration, 0.04 mol.L<sup>-1</sup>.

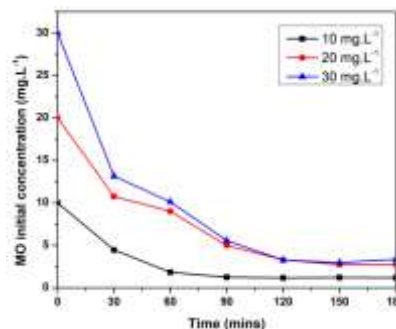


Fig. 8. Effect of MO initial concentration on the degradation efficiency of MO: Ag/ZIF-67 dose, 0.2 g.L<sup>-1</sup>; initial pH 7, temperature, 30°C and H<sub>2</sub>O<sub>2</sub> concentration, 0.04 mol.L<sup>-1</sup>.

The effect of H<sub>2</sub>O<sub>2</sub> concentration was investigated in the range from 0.02 mol.L<sup>-1</sup> to 0.1 mol.L<sup>-1</sup>. It was obviously that the MO degradation rate increased when H<sub>2</sub>O<sub>2</sub> concentration increased (Fig. 9.) This trend could be explained that the main agent to MO degradation is  $\cdot\text{OH}$  radicals produced from H<sub>2</sub>O<sub>2</sub> decomposition. The enhancement of H<sub>2</sub>O<sub>2</sub> could supply more  $\cdot\text{OH}$  radicals leading to the observation for the higher mineralization of MO at higher H<sub>2</sub>O<sub>2</sub> concentration.

It also found that the degradation rates of MO were 72.5%, 88.2% and 98.5% within 180 min in presence of H<sub>2</sub>O<sub>2</sub> concentration of 0.02, 0.04 and 0.06, respectively. Whereas, the degradation efficiency equilibrium was approximately 100% with the H<sub>2</sub>O<sub>2</sub> concentration of 0.08 and 0.1 mol.L<sup>-1</sup> within 60 first min (Fig. 9). Therefore, in this study, the H<sub>2</sub>O<sub>2</sub> initial concentration 0.08 mol.L<sup>-1</sup> was selected as the optimal value when MO initial concentration was 10 mg.L<sup>-1</sup> within 60 min.



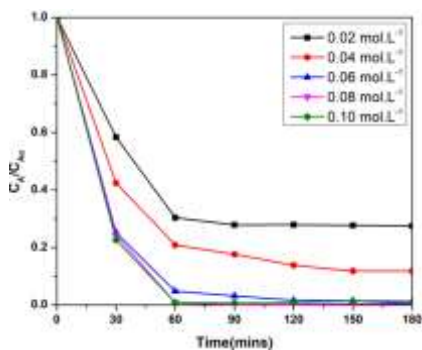


Fig. 9. Effect of  $H_2O_2$  concentration on the degradation efficiency of MO: initial MO,  $10\text{ mg.L}^{-1}$ ; Ag/ZIF-67 dose,  $0.2\text{ g.L}^{-1}$ ; initial pH 7 and temperature,  $30^\circ\text{C}$ .

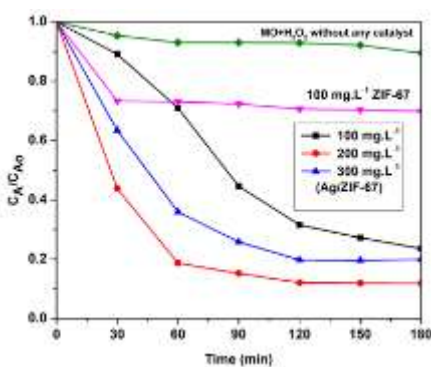


Fig. 10. Effect of Ag/ZIF-67 dose on the degradation efficiency of MO: initial MO concentration,  $10\text{ mg.L}^{-1}$ ; initial pH 7, temperature,  $30^\circ\text{C}$  and  $H_2O_2$  concentration,  $0.04\text{ mol.L}^{-1}$ .

Series of experiments were performed to investigate the effects of Ag/ZIF-67 dose on the degradation efficiency. As shown in Fig. 10, generally, Ag/ZIF-67 would be limited factor. Specially, the degradation efficiency was found to be 76.4%, 88.2% and 80% within 180 min, respectively, when using Ag/ZIF-67 dose of  $100\text{ mg.L}^{-1}$ ,  $200\text{ mg.L}^{-1}$  and  $300\text{ mg.L}^{-1}$ . As the reaction occurred at the  $\text{Ag}^0\text{-H}_2\text{O}_2$  site  $^\circ\text{OH}$  radicals was generated. Increasing dose of material would supply more active site and support the analysis. However,  $^\circ\text{OH}$  could attack  $H_2O_2$  as Eq (2), therefore, it would reduce degradation efficiency. Figure 10 also illustrated that  $H_2O_2$  had low degradation efficiency in 10.5% within 180 min without any catalyst. Using ZIF-67 as a catalyst the efficiency was found 30.2% within 180 min and the material was decomposition at the first use.

### C. Reused Capacity

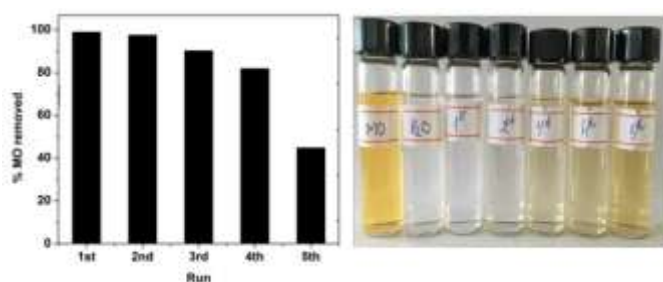


Fig. 11 The MO degradation efficiency after 5 times reused: initial MO,  $10\text{ mg.L}^{-1}$ ; Ag/ZIF-67 dose,  $0.2\text{ g.L}^{-1}$ ; initial pH 7 and temperature,  $30^\circ\text{C}$  and  $H_2O_2$  concentration,  $0.08\text{ mol.L}^{-1}$ .

The recycling performance of the Ag/ZIF-67 was studied by series experiment after five times reused. Figure 11 showed that Ag/ZIF-67 exhibited high durability. However, the efficiency gradually decrease after each time, for instance, efficiency was found 99.6%, 97.52%, 90.23%, 81.9%, 44.6%, respectively for the first, the second, the third, the fourth and the fifth use. Besides, after reused three times, Ag/ZIF-67 was characterized by PXRD and FT-IR (Fig.12). This material was retain all clear peaks at  $38^\circ$ ,  $44^\circ$ ,  $64^\circ$  and  $77^\circ$  (Fig. 12a). The FT-IR spectrum (Fig. 12b) had a similar result, the spectrum of material reused unremarkable change compared with fresh material. The MO degradation efficiency was still over 90% after three times reused.

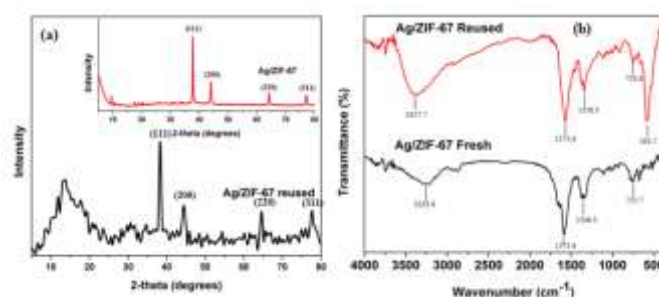


Fig. 12. PXRD pattern and FT-IR spectrum of Ag/ZIF-67 after three times reused

## IV. CONCLUSION

In summary, the Ag/ZIF-67 was successfully synthesized by solution impregnation method between  $\text{AgNO}_3$  salt and ZIF-67 in acetone. The synthesized material had outstanding physicochemical properties and high catalytic activity. High efficiency in degradation of MO was obtained with over 99% when using  $H_2O_2$  concentration  $0.08\text{ mol.L}^{-1}$ , MO concentration  $10\text{ mg.L}^{-1}$ , Ag/ZIF-67 concentration  $200\text{ mg.L}^{-1}$  at  $30^\circ\text{C}$ , pH 7 in 180 min. The solid catalyst could be facily separated from the reaction mixture by simple centrifugation, and could be reused three times without a significant degradation in catalytic activity. This work would provide a new potential technique for treatment of non-biodegradable dye in wastewater.

## ACKNOWLEDGEMENTS

This study is funded in part by the Can Tho University Improvement Project VN14-P6, supported by a Japanese ODA loan. L. T. A. Thur is grateful to Can Tho University through project TSV2019-12.

## REFERENCES

- [1] C. Rösler, and R. A. Fischer, "Metal-organic frameworks as hosts for nanoparticles", *CrystEngComm-Royal Society of Chemistry*, vol. 17, issue 2, pp. 199-217, 2015.
- [2] Y. Pan, Y. Liu, G. Zeng, L. Zhao, and Z. Lai, "Rapid synthesis of zeolitic imidazolate framework-8 (ZIF-8) nanocrystals in an aqueous system", *Chemical Communications*, vol. 47, issue 7, pp. 2071-2073, 2011.
- [3] R. Banerjee, A. Phan, B. Wang, C. Knobler, H. Furukawa, M. O'keeffe, and O. M. Yaghi, "High-throughput synthesis of zeolitic imidazolate frameworks and application to  $\text{CO}_2$  capture", *Science*, vol. 319, issue 5865, pp. 939-943, 2008.
- [4] K. S. Park, Z. Ni, A. P. Côté, J. Y. Choi, R. Huang, F. J. Uribe-Romo, H. K. Chae, M. O'Keeffe, and O. M. Yaghi, "Exceptional chemical and

- thermal stability of zeolitic imidazolate frameworks", *Proceedings of the National Academy of Sciences*, vol. 103, issue 27, pp. 10186-10191, 2006.
- [5] M. Meilikhov, K. Yusenko, D. Esken, S. Turner, G. V. Tendeloo, and R. A. Fischer, "Metals@ MOFs—loading MOFs with metal nanoparticles for hybrid functions", *European Journal of Inorganic Chemistry*, vol. 2010, issue 24, pp. 3701-3714, 2010.
- [6] H.C. Li, W. J. Liu, H. X. Han, and H. Q. Yu, "Hydrophilic swellable metal–organic framework encapsulated Pd nanoparticles as an efficient catalyst for Cr (VI) reduction", *Journal of Materials Chemistry A*, vol. 4, issue 30, pp. 1080-1087, 2016.
- [7] A. K. Singh, and Q. Xu, "Metal–Organic Framework Supported Bimetallic Ni- Pt Nanoparticles as High-performance Catalysts for Hydrogen Generation from Hydrazine in Aqueous Solution", *ChemCatChem*, vol. 5, issue 10, pp. 3000-3004, 2013.
- [8] D. Esken, S. Turner, O. I. Lebedev, G. V. Tendeloo, and R. A. Fischer, "Au@ ZIFs: stabilization and encapsulation of cavity-size matching gold clusters inside functionalized zeolite imidazolate frameworks, ZIFs", *Chemistry of Materials*, vol. 22, issue 23, pp. 6393-6401, 2010.
- [9] T. T. Dang, Y. Zhu, J. S. Ngiam, S. C. Ghosh, A. Chen, and M. Seayad, "Palladium nanoparticles supported on ZIF-8 as an efficient heterogeneous catalyst for aminocarbonylation", *Acs Catalysis*, vol. 3, issue 6, pp. 1406-1410, 2013.
- [10] P. Z. Li, K. Aranishi, and Q. Xu, "ZIF-8 immobilized nickel nanoparticles: highly effective catalysts for hydrogen generation from hydrolysis of ammonia borane", *Chemical Communications*, vol. 48, issue 26, pp. 3173-3175, 2012.
- [11] S. Ding, C. Zhang, Y. Liu, H. Jiang, and R. Chen, "Selective hydrogenation of phenol to cyclohexanone in water over Pd@ N-doped carbons derived from ZIF-67: Role of dicyandiamide", *Applied Surface Science*, vol. 425, pp. 484-491, 2017.
- [12] H. Yang, X. W. He, F. Wang, Y. Kang, and J. Zhang, "Doping copper into ZIF-67 for enhancing gas uptake capacity and visible-light-driven photocatalytic degradation of organic dye", *Journal of Materials Chemistry*, vol. 22, issue 41, pp. 21849-21851, 2012.
- [13] W. Meng, Y. Wen, L. Dai, Z. He, and L. Wang, "A novel electrochemical sensor for glucose detection based on Ag@ ZIF-67 nanocomposite", *Sensors and Actuators B: Chemical*, vol. 260, pp. 852-860, 2018.
- [14] A. Dhakshinamoorthy, and H. Garcia, "Catalysis by metal nanoparticles embedded on metal–organic frameworks", *Chemical Society Reviews*, vol. 41, issue 15, pp. 5262-5284, 2012.
- [15] W. T. Xu, L. Ma, F. Ke, F. M. Peng, G. S. Xu, Y. H. Shen, J. F. Zhu, G. L. Qui, and Y. P. Yuan, "Metal–organic frameworks MIL-88A hexagonal microrods as a new photocatalyst for efficient decolorization of methylene blue dye", *Dalton Transactions*, vol. 43, issue 9, pp. 3792-3798, 2014.
- [16] A. Mittal, A. Malviya, D. Kaur, J. Mittal, and L. Kurup, "Studies on the adsorption kinetics and isotherms for the removal and recovery of Methyl Orange from wastewaters using waste materials", *Journal of Hazardous Materials*, vol. 148, issue 1-2, pp. 229-240, 2007.
- [17] E. Guivarch, S. Trevin, C. Lahitte, and M. A. Oturan, "Degradation of azo dyes in water by electro-Fenton process", *Environmental Chemistry Letters*, vol. 1, issue 1, pp. 38-44, 2003.
- [18] E. Brillas, I. Sirés, and M. A. Oturan, "Electro-Fenton process and related electrochemical technologies based on Fenton's reaction chemistry", *Chemical Reviews*, vol. 109, issue 12, pp. 6570-6631, 2009.
- [19] S. Haji, B. Benstaali, and N. Al-Bastaki, "Degradation of methyl orange by UV/H<sub>2</sub>O<sub>2</sub> advanced oxidation process", *Chemical Engineering Journal*, vol. 168, issue 1, pp. 134-139, 2011.
- [20] J. Shao, Z. Wan, H. Liu, H. Zheng, T. Gao, M. Shen, Q. Qu, and H. Zheng, "Metal organic frameworks-derived Co<sub>3</sub>O<sub>4</sub> hollow dodecahedrons with controllable interiors as outstanding anodes for Li storage", *Journal of Materials Chemistry A*, vol. 2, issue 31, pp. 12149-12200, 2014.
- [21] S. A. Babu, and H. G. Prabu, "Synthesis of AgNPs using the extract of Calotropis procera flower at room temperature", *Materials Letters*, vol. 65, issue 11, pp. 1675-1677 2011.
- [22] K. Y. A. Lin, and H. A. Chang, "Ultra-high adsorption capacity of zeolitic imidazole framework-67 (ZIF-67) for removal of malachite green from water", *Chemosphere*, vol. 139, pp. 624-631, 2015.
- [23] A. F. Gross, E. Sherman, and J. J. Vajo "Aqueous room temperature synthesis of cobalt and zinc sodalite zeolitic imidizolate frameworks", *Dalton Transactions*, vol. 41, issue 18, pp. 5458-5460, 2012.
- [24] J. Z. Guo, H. Cui, W. Zhou, and W. Wang, "Ag nanoparticle-catalyzed chemiluminescent reaction between luminol and hydrogen peroxide", *Journal of Photochemistry and Photobiology A: Chemistry*, vol. 193, issue 2-3, pp. 89-96, 2008.